

# Grain growth and recrystallization of nanocrystalline $\text{Al}_3\text{Ti}$ prepared by mechanical alloying

F. ZHANG, L. LU, M. O. LAI

*Department of Mechanical Engineering, The National University of Singapore, Singapore 119260*

*E-mail: mpeluli@nus.edu.sg*

F. H. (SAM) FROES

*Department of Metallurgy, Mining and Geological Engineering, University of Idaho*

The grain sizes and lattice strains during mechanical alloying of Ti-75 at.% Al powder mixtures were studied using X-ray diffraction methods. Nanocrystalline  $\text{L}_{12}\text{-Al}_3\text{Ti}$  was obtained after a certain time period of ball milling. Minimum grain sizes of 17 nm for Al and 28 nm for Ti have been determined using XRD. During subsequent thermal annealing processing, an obvious recrystallization resulting in significant reduction of grain size was observed. The recrystallization in nanocrystalline  $\text{Al}_3\text{Ti}$  was affected by both the temperature and the degree of order. The incubation period for recrystallization at 400°C was about 6 hours while those at 510 and 700°C were about 2 hours. The completion time of recrystallization in  $\text{Al}_3\text{Ti}$  at 400 and 700°C was about 15 hours and 8 hours at 510°C. It is clear that the recrystallization at 700°C was retarded as a result of the higher degree of order structure which limited the mobility of the boundaries. Phase transformation occurring within the recrystallization temperature range was observed to have little influence on the recrystallization itself. However, transformation products do have significant effects on it which is originated from the degree of order in the products. The recrystallization in this alloy system provides an excellent means to maintain the nanocrystalline microstructure during the necessary consolidation thermal cycle by decreasing the processing temperature and increasing the hold time considerably. © 2003 Kluwer Academic Publishers

## 1. Introduction

Intermetallic compounds, especially titanium aluminides, are regarded as one of the most promising candidates for aerospace structural materials in the 21<sup>st</sup> century due to their low density combined with good mechanical properties and corrosion resistance at medium high temperature range [1]. Among the titanium aluminides,  $\text{Al}_3\text{Ti}$  is the lightest with a density of about 3.3 g/cm<sup>3</sup>. The brittleness at low temperature, however, is by far the greatest hurdle that prevents the titanium trialuminides from being widely used in industrial applications [2].

Nanocrystalline materials are novel materials that are not only scientifically interesting but also hold great potential for varied applications. They are polycrystalline materials with grain size of up to about 100 nm in at least one dimension. It has been shown that by decreasing the grain size to nanometer levels, traditionally soft and ductile metals can be made very hard and strong, and conventional ceramics that are brittle can be made to deform plastically like metals. The enhanced diffusivity in these materials results in increased solubility, and ease in synthesis of alloy phases from normally difficult

alloyed metals and also allows the sintering of powder compacts at temperatures much lower than those required for coarse grained polycrystalline materials.

Because of the very fine grain size, nanocrystalline materials exhibit a variety of properties that are different and often considerably improved in comparison with those of conventional coarse-grained polycrystalline materials. These include increased strength/hardness, reduced density, reduced elastic modulus, high electrical conductivity, increased specific heat, higher thermal expansion coefficient, lower thermal conductivity, and superior soft magnetic properties [3].

Recent researches [4,5] showed that reducing the grain size to nanometer range may be a possible means to improve the ductility of intermetallics, providing the nano-sized grains can be maintained at application temperatures. This is because deformation mode by conventional dislocation generation and motion may not happen in such small grains; instead, deformation by diffusion controlled mechanism is expected [3]. According to reference [6], the calculated volume fraction of grain boundaries can reach as high as 30–40% in nanocrystalline materials of grain size in the range of

2–3 nm. Such a large fraction of grain boundaries can serve as fast diffusion path [7], and a change in deformation mode from slip to that like Coble creep may be expected.

Nanocrystalline materials can be produced by techniques such as mechanical alloying, gas condensation, and electrodeposition etc. In this study, mechanical alloying is employed to fabricate nano-sized titanium tri-aluminides powders. Since the nanocrystalline materials possess a large fraction of interfacial regions and therefore are in a high-energy non-equilibrium state, grain growth will inevitably occur to decrease the interfacial energy and hence the total energy of the system during the exposure to high temperature when the powders are subsequently consolidated into bulk materials of a sizable dimension by HIP or other methods. On the other hand, the high density of dislocations generated during MA will provide the driving force for recrystallization to take place in the MAed materials. This will also provide a means of grain refinement for the alloy. Therefore, a thorough understanding of grain growth and its kinetics of these nanocrystalline materials is of great importance. In the present paper, the evolution in grain size and lattice strain of Ti-75Al powders during MA is investigated. Grain growth and kinetics of the MAed Ti-75Al powders at different temperatures are also studied.

## 2. Experimental procedures

Commercially pure Ti (99.9%) and Al (99.98) powders with particle size less than 150  $\mu\text{m}$  were used as the starting materials. The powders in the stoichiometric composition of Ti-75at.%Al were mixed and blended in a V-blender for 3 hours before ball milling. Ball milling was carried out in a Frisch 5 Planetary ball mill with stainless steel vials and balls. 20 grams of the powder mixture was loaded for each batch of milling. The ball to powder weight ratio in this study was fixed at 20 : 1. In order to prevent contamination from the atmosphere, the charged vial was evacuated by a vacuum pump for 30 minutes and then filled with purified Argon gas. 3 wt% of stearic acid [ $\text{CH}_3(\text{CH}_2)_{16}\text{CO}_2\text{H}$ ] was added as process control agent (PCA) to prevent agglomeration of the powders during milling.

The structure of the powders was determined by a Lab 6000 SHIMADZU X-ray diffractometer using  $\text{Cu K}\alpha$  radiation ( $\lambda = 1.5406 \text{ \AA}$ ). To precisely calculate the grain size and the lattice strain of the milled powders, a step scan mode with scanning step of 0.02 degree and preset time of 2 second was utilized. A Rheometric<sup>TM</sup> STA 1500 thermal analyzer was used to measure the transition temperature and enthalpies of the ball milled powders at a heating rate of 20°C/min. The melting transitions of pure indium and gold were used as the temperature and enthalpy calibration standards of the thermal analyzer.

Grain size  $D$  of the MAed powders was determined from the broadening of the x-ray diffraction profiles using Williamson-Hall's equation [8]:

$$B \cos \theta_B = 0.9\lambda/D + 2\varepsilon \sin \theta_B$$

where  $B$  is the broadening of the profile,  $\theta_B$ , the Bragg angle,  $\lambda$ , the wavelength of the radiation and  $\varepsilon$ , the lattice strain factor.  $D$  may be determined by extrapolating the straight line plot of  $B \cos \theta_B$  versus  $\sin \theta_B$  to  $\sin \theta_B = 0$ , while the strain factor  $\varepsilon$  may be obtained from the gradient of the same straight line.

Isochronal and isothermal annealing were applied to the MAed powders to investigate grain growth kinetics.

## 3. Experimental results and discussions

### 3.1. Evolution grain size during ball milling

The evolution in grain size of Al is listed in Table I and is graphically shown in Fig. 1. The variation in grain-size of Al can be divided into four stages. Within 1 hour of milling, the grain size of Al decreases rapidly from 492 nm to 206 nm. The grain size then remains almost unchanged for up to 5 hours of milling, as can be seen from the plateau shown in Fig. 1a. Continuous milling causes the grain size to be reduced to tens of nanometers. Grain size of the sample milled for 10 hours is about 84 nm, which is much smaller than that for the 5-hour sample of 202 nm. The decrease in grain size

TABLE I Ti-75Al: Grain size and strain data of Al

Ball milling time (hrs)	Grain size (nm)	Strain (%)
0	492.	0.1
1	206	0.03
5	203	0.2
10	84	2.1
15	26	1.7
20	17	0.6
30 (new phase)	22	0.8
40 (new phase)	18	0.6

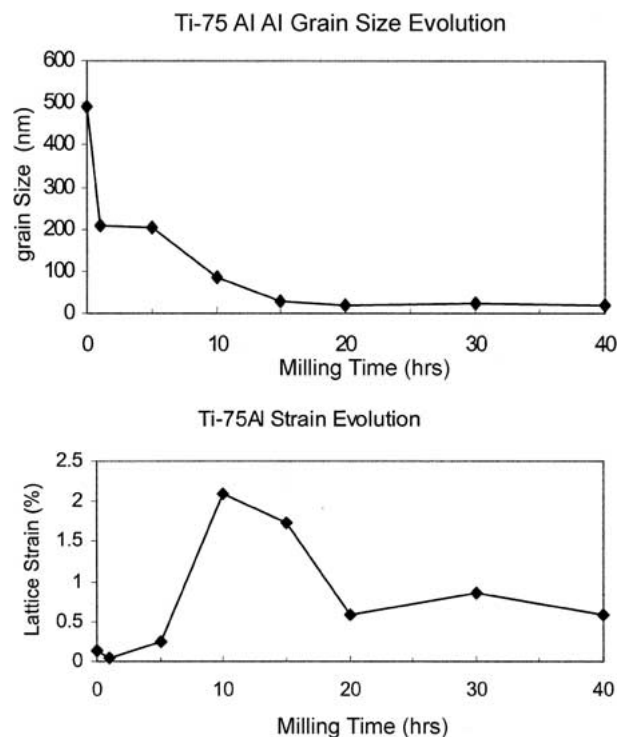


Figure 1 Grain size and lattice strain of Al after different times of milling.

continues gradually until 20 hours of milling when it becomes stable. Further milling results in the formation of  $L1_0$ - $Al_3Ti$  intermetallic compound [9]. Grain size of the newly formed phase is of the order of 20 nm, which is close to that of the Al powder after 20 hours of milling.

The lattice strains in the ball-milled Al powders, also listed in Table I and shown in Fig. 1b, peak at 10 hours of milling. Accumulated in a slow rate before 10 hours of milling, it reaches as high as 2.1% after 10 hours of milling and slightly decrease to 1.7% at 15 hours. Further milling resulted in a fast release of strain in the lattice range. It is interesting to note that the highest strain occurred when the grain size is reduced sharply to less than 100 nm. With further release in lattice strain, the grain size remained essentially unchanged. It is therefore reasonable to relate the grain size obtained with the lattice strain accumulated in the material.

Grain sizes and lattice strains of the Ti powders are calculated and listed in Table II, and graphically shown in Fig. 2.

TABLE II Ti-75Al: Grain size and strain data of Ti

Ball milling time (hrs)	Grain size (nm)	Strain (%)
0	289	0.2
1	384	0.6
5	213	0.5
10	54	1.2
15	29	0.6
20	28	1.2

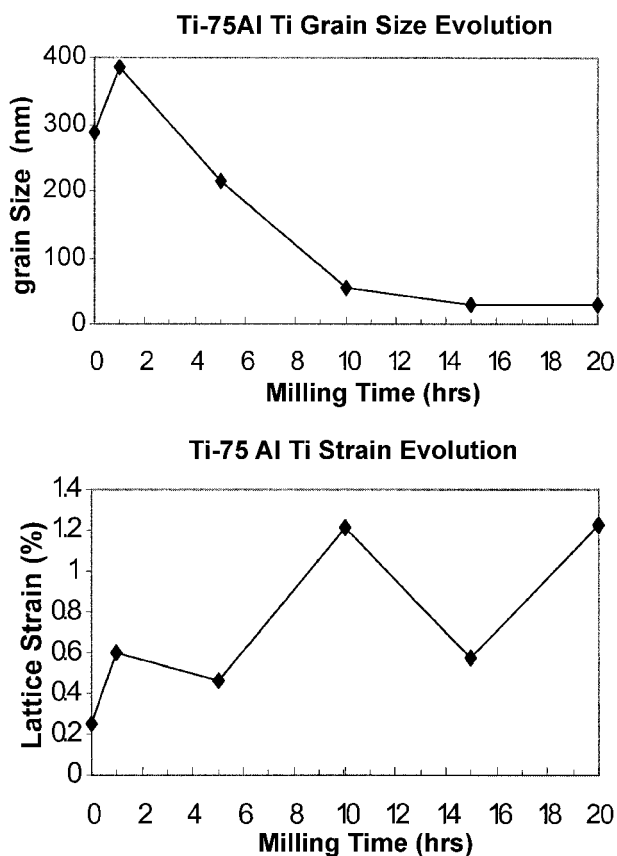


Figure 2 Grain Size and lattice strain of Ti after different times of milling.

Since diffraction peaks of Ti disappear after 20 hours of milling, the calculations could only be extended to 20 hours. From Table II, it can be observed that the grain size of Ti continuously decreases with milling time. For the 15 hour milled sample the rate of reduction in grain size becomes flat after the grain size has reached 29 nm. It can be estimated that the refinement process would continue since only 6.7 wt% of the Ti has been found to be solid solutionized in Al after 20 hours of milling [9].

The highest strain level in the Ti lattice was found to be 1.2% and between 10 and 20 hours of milling. The values of peak lattice strain are lower than those of Al of about 2.1%.

A lower limit for grain sizes appears to exist for both Al and Ti powders under the present ball milling condition. The  $d_{min}$  (Al) is about 20 nm while  $d_{min}$  (Ti), about 30 nm. It is interesting to note that the grain size of Ti with less ductility (hcp structure) was larger than that of very ductile Al (fcc structure). It is generally accepted that ductile materials are not easily fractured and hence difficult to achieve very small grain size. The intrinsic nature of grain size reduction in MA is the continuous fracturing of the milled powders. The continuous fracturing results in the breaking of the powder particles and therefore the grain boundaries of the materials. Soft powder particles tend to stick to the wall of ball-milling vials and are not easy to be fractured. Consequently, the refinement process in ductile material is usually not as fast as brittle material.

It has been shown [10] that the minimum grain size,  $d_{min}$ , obtainable is related to the structures of the materials. In general,  $d_{min}$  follows the relation:  $d_{min}(FCC) < d_{min}(BCC) < d_{min}(HCP)$ . Another factor to be considered is the existence of minimum inter-spacing  $L$  for the dislocation separation in a pile up originated from the equilibrium between the repulsive force between dislocations and the external applied force,  $L$  is given by [6]:

$$L = \frac{3Gb}{\pi(1 - \gamma)H_v}$$

where,  $G$  is the shear modulus;  $\gamma$ , the Poisson ration;  $b$ , Burgers vector and  $H_v$ , hardness of the material. Using the above equation,  $L_{min}$  (Ti) can be evaluated at about 30 nm, while  $L_{min}$  (Al), about 75 nm. Therefore, minimum grain size of relative brittle Ti of 28 nm in the present study is very close to its  $L_{min}$  (Ti) while that of Al of 17 nm is much less than  $L_{min}$  (Al). It is estimated that  $L_{min}$  can affect brittle materials more than ductile materials.

### 3.2. Evolution of grain size during thermal treatment

One crucial aspect of nanocrystalline materials is grain growth since the material is in a metastable state and has the tendency for grain growth. The desired properties of the materials are eliminated once the grains have grown to certain sizes. It is therefore important to investigate the grain growth phenomenon and its kinetics in nano-sized materials.

Grain size of the Ti-75Al powders ball milled for different time durations after annealing at 900°C are

shown in the Table III and Fig. 3. It can be observed that after heating up to 900°C, grain sizes in almost all the samples are approximately the same except for samples milled for 15 hours, irrespective of the initial grain sizes. The grains have reached a size as high as 227–265 nm after exposure to 900°C.

To investigate grain growth of the ball milled Ti-75Al powders at high temperature, samples milled for 10 and 30 hours were annealed at different temperatures for 1 hour. The results are shown in Tables IV and V and Figs 4 and 5.

For the sample milled for 10 hrs, the grain size can be seen to increase rapidly over the entire temperature range studied. Comparing with the sample milled for 10 hours, it is found that grain growth for samples milled for 30 hours, occurred very slowly at temperature

TABLE III Evolution of Ti-75Al grain size at high temperature

Milling time (hrs)	As milled (nm)	900°C (nm)
1	206	260
5	203	247
10	84	237
15	26	138
20	17	227
30	22	265
40	18	----

TABLE IV Grain size evolution of Ti-75Al sample milled for 10 hours after exposing to different temperatures for 1 hour

Annealing temp. (°C)	Grain size (nm)	Standard deviation (nm)
Room temp.	84	6.8
400	124	15.8
500	188	26.5
650	143	14.4
900	237	77.4

TABLE V Grain size evolution of Ti-75Al sample milled for 30 hours after exposing to different temperatures for 1 hour

Anneal temp. (°C)	Grain size (nm)	STDEV
Room temp.	22	3.6
500	82	15.8
600	51	22.4
700	103	18.7
800	43	12.5
900	265	27.3

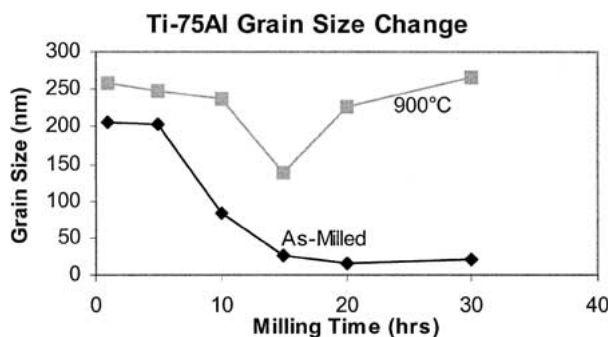


Figure 3 Ti-75Al changes in grain size after annealing at 900°C.

TABLE VI Grain sizes (nm) of sample milled for 30 hours after isothermal annealing for different times

Annealing time (ks)	Annealing temperature (°C)			
	400		510	700
	L1 <sub>2</sub> -Al <sub>3</sub> Ti	Al <sub>3</sub> Ti	Al <sub>3</sub> Ti	Al <sub>3</sub> Ti
3.6 (1 hr)	24	--	82	161
7.2 (2 hr)	37	44	126	227
14.4 (4 hr)	31	91	105	170
21.6 (6 hr)	70	138	96	162
28.8 (8 hr)	133	130	71	118
54 (15 hr)	--	90	97	114
72 (20 hr)	--	113	97	116

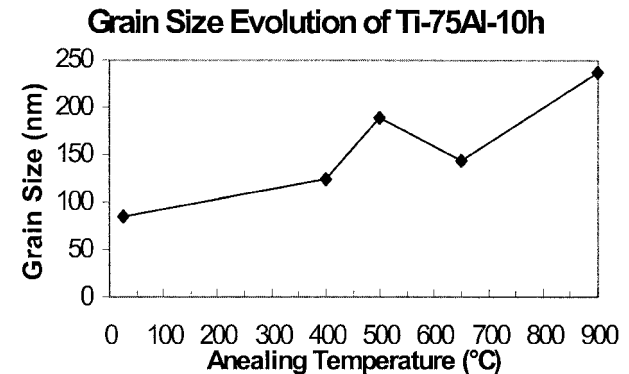


Figure 4 Change of grain size in 10-hour milled Ti-75Al samples after annealing at different temperatures.

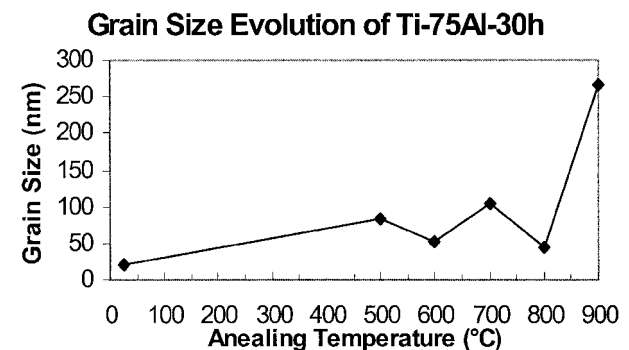


Figure 5 Change of grain size in 30-hour milled Ti-75Al samples after annealing at different temperatures.

below 900°C. The grain size after annealing at 800°C for 1 hour was only 43 nm, well below 100 nm. However, when the heat-treatment temperature was increased to 900°C, the grains grew at a very fast rate and reached as high as 265 nm eventually. The interesting point here is that the grain sizes treated at 600°C and 800°C are clearly smaller than those treated at 500°C and 700°C respectively, which is contradicted to our normal reasoning. These phenomena could be due to the recrystallization during isothermal annealing, and this will be discussed in detail later.

In order to investigate the kinetics of grain growth, the sample MAed for 30 hours were isothermally annealed at different temperatures for different times and the results are listed in Table VI and Fig. 6.

The evolution of grain size during isothermal heat-treatment can be divided into three stages. At the early

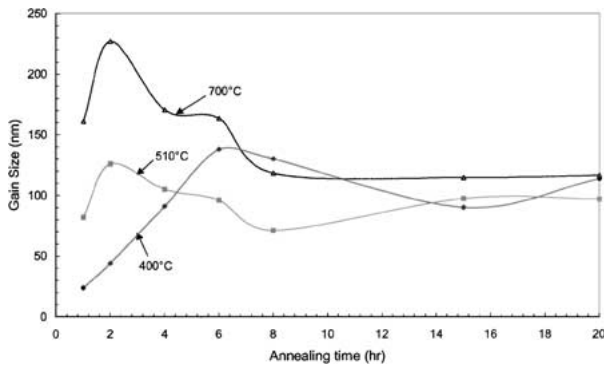


Figure 6 Grain size evolution in 30-hour milled sample after different annealing conditions.

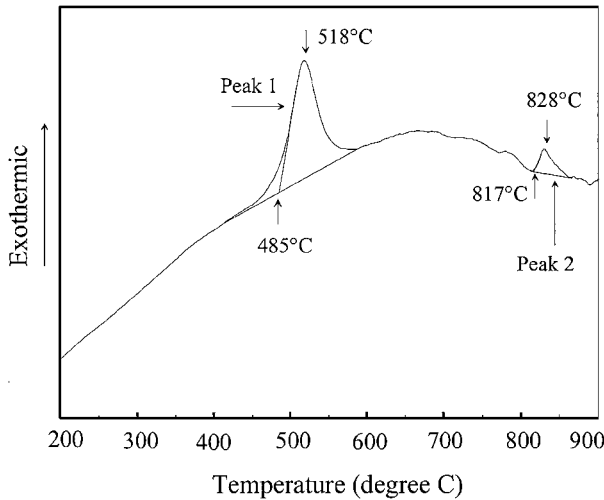


Figure 7 DTA result of sample milled for 30 hours.

stage of annealing, grain size increases with time. However, prolonged exposure at high temperature results in obvious decrease (refinement) in the grain size. After the second stage the grain manifests a slight tendency to grow.

The decrease in grain size is usually associated with recrystallization or formation of a new phase. To investigate the nature of this result, the reaction kinetics was investigated. Results of thermal analysis of the sample milled for 30 hrs are shown in Fig. 7. As shown in our previous study [9], the first peak is due to the allotropic transformation from  $L1_2$ - $Al_3Ti$  to  $D0_{23}$ - $Al_3Ti$ , while the second peak,  $D0_{23}$ - $Al_3Ti$  to  $D0_{22}$ - $Al_3Ti$ . These two reactions are kinetic restrained reactions with activation energy of 147 and 243 kJ/mol respectively. For such reaction, Arrhenius equation is satisfied:

$$K = K_0 \exp(Q/RT^2), \text{ while } dX/dt = K(1 - X)^n$$

where  $X$  is the percentage of phase already transformed,  $t$  is the duration of annealing. Since the allotropic transformation is a first order reaction,  $n = 1$ .  $X$  can therefore be expressed as:  $X = 1 - \exp(-1/Kt)$ . Using the above equations, transformation kinetics as a function of annealing time and temperature is plotted in Fig. 8a and b. The three annealing temperatures chosen for the present study were  $T_1$  (510°C) =  $T_{max}$  of peak 1,  $T_2$  (400°C) <  $T_{max}$  and  $T_3$  (700°C) >  $T_{max}$ .

It can be seen that at 400°C, transformation from  $L1_0$  to  $D0_{23}$  ended at about 7 hours of annealing (Fig. 8a) which coincides with the time when the grains size reaches the peak as shown in Fig. 6. The allotropic transformation did not induce a decrease in the size of the grain, which means that the newly formed grains were relatively larger in dimensions. The allotropic transformation in  $Al_3Ti$  can be achieved by influencing the anti-phase boundary (APB) energy on the cube planes. For example, the tetragonal  $D0_{22}$  structure can be obtained from the cubic  $L1_2$  structure by displacing every other (001) plane by a vector of  $\frac{1}{2}$  [110] [11]. In addition, no finer grain size can be observed during the transformation process, which implies that no new nuclei were observed during the transition. It can therefore be hypothesized that the allotropic transformation occurred without a nucleation process and directly in the original  $L1_2$  lattice. The same conclusion can also be obtained from samples annealed at 510°C and 700°C. From Fig. 8b it can be seen that after 2 hours of annealing,  $D0_{23}$ - $Al_3Ti$  to  $D0_{22}$ - $Al_3Ti$  transition was 80% completed at 700°C, while grain growth occurs in a normal way as shown in Fig. 6. If the allotropic reaction had been nucleation controlled, smaller new phase grains should be observed before 2 hours of annealing. As no such phenomenon can be found in the present study, it can be concluded that the two allotropic reactions themselves had little effects on the grain refinement of  $Al_3Ti$ .

It was observed that the grain size of  $Al_3Ti$  annealed at various temperatures generally increased initially reaching a maximum before it decreased gradually. However, it should be noted that at grain size peaks after 6 hours of annealing at 400°C, while only 2 hours at 510 and 700°C.

The decreasing trend in the  $Al_3Ti$  system may be attributed to the recrystallization process during annealing. In general, this is a process to decrease the internal energy in the heavily deformed materials to eliminate high-density dislocations and to nucleate new strain-free grains. The mechanically alloyed powders in the present study could be considered as heavily deformed metals since the relatively ductile Al and Ti were subjected to severe plastic deformation due to the continuous impacting and shearing forces during ball milling. The milled powders therefore inevitably experience the recovery and recrystallization process during subsequent thermal annealing. The driving force for these two processes is the increased Gibbs free energy in the system:  $\Delta G = \Delta E - T\Delta S$ . Since ball milling is essentially a room temperature process,  $\Delta S$  during the process is negligible in comparison with  $\Delta E$ . Consequently the increased internal energy  $\Delta E$  becomes the driving force for recovery and recrystallization.  $\Delta E$  usually originates from the introduction of high density of dislocations during the milling process.

The density of dislocations in the deformed materials can be roughly estimated using the following equation [12]:

$$\rho = \varepsilon/(L^*b)$$

where  $\rho$  is the density of dislocation with Burgers Vector  $b$ ,  $\varepsilon$  is the strain accumulated during ball milling,

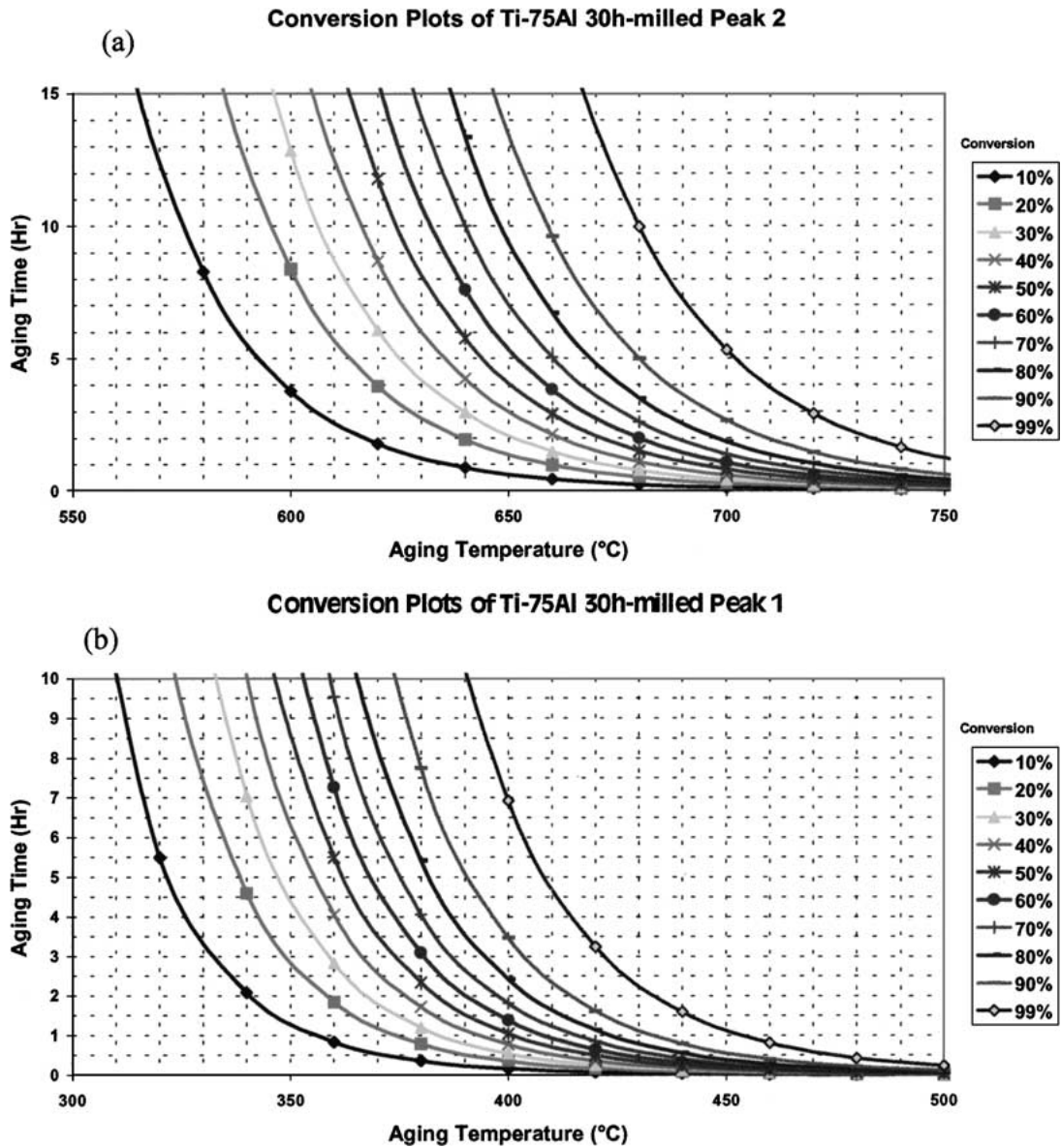


Figure 8 Transformation percentage at different annealing temperature and annealing time for peak 1 (a), and peak 2 (b).

and  $L$ , the average moving distance of dislocations. Since the crystalline size here is very small after long period of milling, it can be assumed that this size is equal to  $L$ .

The average lattice strain of  $L_{12}$ - $Al_3Ti$  shown in Table I is about 0.8%, which is very close to that obtained by Kawanishi *et al.* [13] in intermetallic compound niobium aluminides, and the crystalline size, about 22 nm. Using these data, it can be estimated that the dislocation density in the sample milled for 30 hours is about  $8 \times 10^{16}/m^2$ . The increased dislocation density is due to the continuous trapping of newly formed mobile dislocations by existing dislocations and their incorporation into different microstructural features such as low angle grain boundaries which form the walls of the subgrains. In addition, using the model proposed by Suryanarayana *et al.* [6], it can be estimated that the volume percentage of grain boundaries in the alloy with a grain size of 22 nm can reach as high as 15%. Both the high density of dislocation and the large amount of grain boundaries can provide the driving force for the recrystallization observed in this study.

It was found that the recrystallization in the present study has a clearly identified incubation period. The duration of this period was governed by both the annealing temperature and the ordered structure. At 400°C, the incubation period was as long as 6 hours, while with the increase in treating temperature, it was shortened to about 2 hours at 510°C and 700°C. The incubation period observed during isothermal annealing refers to the average time required for a series of thermally activated fluctuations to form a strain-free region equal to, or larger than the critical size for stability. It may be observed from the present study that the nuclei in the recrystallization have not been formed in the strict thermodynamic sense, but are caused by a strain induced grain boundary migration (SIBM). Since the nucleation is a kinetic restrain process, higher temperature will facilitate the mobility of dislocation and promote the formation of nuclei. The increase in treatment temperature will therefore shorten the incubation period.

As shown in Table VI, the incubation periods at 510°C and 700°C are the same, both about 2 hours,

which implies that the nucleation process at a relatively high temperature of 700°C was nearly the same as that at 510°C. It may also be concluded that the onset of recrystallization at 700°C was retarded. If the atomic order is considered, it can be found that the degree of order in the alloy has increased after the transformation from L1<sub>2</sub>-Al<sub>3</sub>Ti to D0<sub>23</sub>-Al<sub>3</sub>Ti at 510°C or transition from D0<sub>23</sub>-Al<sub>3</sub>Ti to D0<sub>22</sub>-Al<sub>3</sub>Ti at about 817°C. The degree of order in the alloy can influence the mobility of the grain boundary, which in turn will affect both the nucleation rate and grain growth itself. Although the second reaction temperature at 817°C was not attained in the present isothermal treatment, the kinetic study shown in Fig. 8 does show that after 2 hours of annealing 80% of the original phase has been transformed to D0<sub>22</sub>-Al<sub>3</sub>Ti which possesses the highest degree of order. This higher degree of order arrangement of the atoms in the alloy was assumed to be the main reason for the retardation of the recrystallization process.

Here it can be found that two main factors tend to influence the onset of recrystallization in the present Al<sub>3</sub>Ti system, namely, heat-treatment temperature and the degree of order of the alloy. It can be found from Fig. 8 that D0<sub>23</sub>-Al<sub>3</sub>Ti is the only phase for both the 500 and 600°C treated samples. Under this circumstance, temperature is therefore the only factor that governs the recrystallization process. Higher temperature will accelerate the recrystallization process and reduce the incubation period, that is, recrystallization and decrease in grain size occurred earlier at 600°C. Consequently, in comparison with the normal grain growth at 500°C, the recrystallized sample at 600°C would exhibit smaller grain size. This also explains why the grain size in sample treated at 800°C/1hr is smaller than that treated at 700°C/1hr.

It is interesting to observe the difference between the present nanocrystalline Al<sub>3</sub>Ti system and the traditional recrystallization process with grain size of tens of microns. The original grain size of L1<sub>2</sub>-Al<sub>3</sub>Ti of about 22 nm is very close to that of the nuclei of recrystallization. The critical size of the nucleus,  $R$ , is governed by the interfacial energy  $\gamma_b$  and the strain energy  $E_v$ :  $R > 2\gamma_b/E_v$ . From the calculation of Burke and Turnbull [14], it can be estimated that the minimum nucleus size is within 3 to 50 nm implying that after the formation of nucleus, the growth of it is limited by the original grain boundaries. In addition, since the volume fraction of grain boundaries in the present alloy can reach as high as 15%, as we mentioned before, the preferred nucleation site is much more than for conventional materials and a high nucleation rate may be expected. This also implies that after recrystallization, the grain size is relatively smaller.

#### 4. Conclusions

1. A minimum grain size of 17 nm for Al and 28 nm for Ti was obtained after certain duration of ball milling. The lower limit of grain size in the metals appeared to be originated from the limitation of dislocation separation in a pile up. The L1<sub>2</sub>-Al<sub>3</sub>Ti obtained possessed a grain size of about 22 nm.

2. A decrease in grain size was observed in the samples that had undergone isothermal treatment. The present experimental results indicated that the decrease in grain size was attributed to the recrystallization of the severely cold worked MAed powders during annealing.

3. It could be found in the present study that the annealing temperature and degree of order of the alloy are the main factors that control the incubation period of the recrystallization process. However, the allotropic reaction itself in the recrystallization temperature range had little effect on the recrystallization process.

4. The size of the recrystallization nucleus was in the same order of magnitude as that of MAed L1<sub>2</sub>-Al<sub>3</sub>Ti. This together with the higher dislocation density ( $8 \times 10^{16}/\text{m}^2$ ) and high volume percentage of grain boundaries (15%) was the reason for the large refinement effect during the recrystallization of nanocrystalline materials.

5. Proper control of the recrystallization process provided an effective means to maintain the nanocrystalline microstructure in the MAed materials during subsequent thermal consolidation cycles.

#### References

1. Y. W. KIM, *JOM* **46**(7) (1994) 30.
2. D. VUJIC, Z. X. LI and S. H. WHANG, *Metall. Trans.* **19A** (1988) 2445.
3. S. Q. XIAO, A. H. FOITZIK, G. WELSCH, T. HAUBOLD and H. GLEITER, *Acta Metall. Mater.* **42**(7) (1994) 2535.
4. D. K. KIM and K. OKAZAKI, P/M in Aerospace and Defence Technology, MPIF, Princeton, N.J., 1991, p. 365.
5. H. GLEITER, *J. Appl. Crystallogr.* **24** (1990) 79.
6. S. SURYANARAYANA, D. MUKHOPADHYAY, S. N. PATANKAR and F. H. FROES, *J. Mater. Res.* **7** (1992) 2114.
7. R. BIRINGER and H. GLEITER, in "Encyclopedia of Materials Science and Engineering" edited by R. W. Cahn (Pergamon Press, Oxford, 1988) vol. 1, p. 329.
8. G. K. WILLIAMSON and W. H. HALL, *Acta Metall.* **1** (1952) 22.
9. F. ZHANG, L. LU and M. O. LAI, *J. Alloys & Comp.*, in press.
10. C. C. KOCH, *Nanostruc. Mater.* **9** (1997) 13.
11. H. MABUCHI, K. HIRUKAWA, H. TSUDA and Y. NAKAYAMA, *Scripta Metall.* **24** (1990) 505.
12. M. F. ASHBY, *Phil. Mag.* **21** (1970) 399.
13. S. KAWANISHI, K. ISONISHI and K. OKAZAKI, *Mater. Trans., JIM* **34**(1) (1993) 43.
14. J. E. BURKE and D. TURNBULL, *Prog. Metal Phys.* **3** (1952) 220.

Received 6 June 2000

and accepted 19 July 2001